Leveraging Time Series Imaging Spectrometer Data and Deep Learning for Methane Plume Detection and Delineation

Patrick R. Sullivan[1], Kelly O'Neill[1], Andrew K. Thorpe[2], Riley Duren[3,4], and Philip E. Dennison[1]

[1]University of Utah [2]NASA Jet Propulsion Laboratory, California Institute of Technology, [3]Carbon Mapper, [4]University of Arizona

Background

Atmospheric methane is a powerful greenhouse gas 28 times more powerful than carbon dioxide and responsible for 20% of anthropogenic radiative forcing since 1750.[1,2] Anthropogenic sources contribute 50-65% of methane emissions and are typically underestimated in bottom-up emission budgets.[3] Methane point source emitters follow a heavy-tail distribution, where a handful of "super-emitter" point sources produce 20-50% of a total regional emission budget.[4]

Methane enhancement above background can be detected and quantified in imaging spectroscopy data due to absorption features in the shortwave infrared (SWIR). Matched filters applied to these data are often used to find methane enhancement above background.[5] From pixel enhancements, the Integrated Methane Enhancement (IME) can be derived, which is in turn used to find flux.[6] Delineation of plumes from background and confusers in the matched filter result is required to find IME.[7] Delineation is commonly done using simple statistics or manual identification.

Deep learning is becoming increasingly utilized in remote sensing research and applications.[8] Specifically, convolutional neural networks (CNN) are a powerful tool that can detect local structure and patterns.[9] Fully convolutional networks (FCN) are more flexible and often faster than CNNs and allow for semantic segmentation of an image.[10] FCNs offer the potential to delineate methane plumes on the pixel level accurately, quickly, and without manual input.

Motivation

New and upcoming imaging spectroscopy satellite missions such as PRISMA, Carbon Mapper, and SBG offer new opportunities for repeat observations of point source emitters around the world. While methane plumes are temporally dynamic, confusers producing "false positive" methane detections, such as human-built structures, are typically stationary over time. By training a FCN on time series imaging spectrometer data, we aim to accurately delineate methane plumes from stationary background and confusers without the need for time-intensive manual input.

Instrument and Data Collection

The NASA JPL Airborne Visible/Infrared Imaging Spectrometer Next Generation (AVIRIS-NG) sensor is a pushbroom imaging spectrometer covering a spectral range of 380-2510 nm with bands centered at 5 nm intervals. AVIRIS-NG was repeatedly flown over a controlled release of methane on September 17th, 2018 near Helendale California. 28 flyovers were completed, 18 of which detected methane enhancement. The spatial resolution of the data are 2.3m.

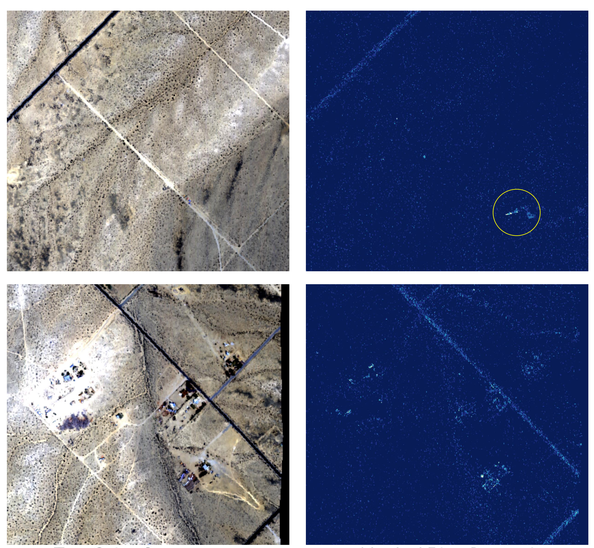

Figure 1. True color composites and macheted filter retrievals of the 2018 time series data. In addition to finding the plume in the top-right tile (yellow circle), the matched filter also identified a variety of roads, roofs, and small portions of desert as false methane enhancements.

Methods

A matched filter algorithm was applied to the time series data to retrieve methane enhancement.[4] Each detected controlled release methane plume was manually labeled. Scenes with matched filter enhancement and red, green and blue radiance channels were used for prediction, while the manually derived labels were used as truth values. Each scene was cropped to tiles of 480x480 pixels. These scenes were then augmented with 50% overlap, horizontal flip, vertical flip, random rotation, and transposed axes to increase the size of the training dataset and the robustness of the network.

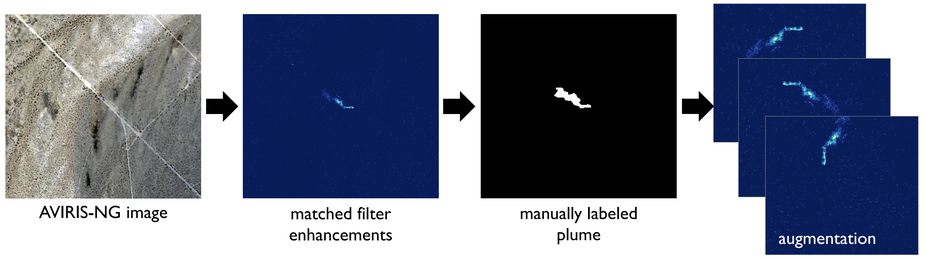

Figure 2. Preprocessing steps before feeding the data into U-Net.

A FCN based on the U-Net architecture was used for semantic segmentation.[10] U-Net allows for a high number of down-sampled feature layers at no cost to image resolution in thanks to a decoder path that mirrors the initial encoder path. The FCN was trained and implemented in python, primarily relying on the TensorFlow, Keras, and NumPy libraries. Fourteen scenes were used for training, while four were used to test the model for an 80/20 split. The model was trained on a Windows 10 virtual workstation with a CPU at 3.09 GHz, 384 GB of installed RAM, and a Nvidia Tesla T4 GPU with 14 GB of dedicated GPU memory. A minibatch of five was used due to processing constraints. Early stopping and reduced learning rate callbacks were used to reduce overfitting. The FCN trained for 2.34 hours and converged due to early stopping after 17 epochs. A prediction confidence of 60% was used as the threshold for assigning a pixel as methane. The IME of both the labeled plumes and the predicted plumes were calculated.

Results and Discussion

The trained FCN successfully delineated methane plumes in the test dataset (Figures 3-4). With a precision of 0.835 and a recall of 0.412, we can characterize the FCN as conservative. The FCN missed more than half of the labeled methane pixels, but the predicted methane pixels were true positives 83.5% of the time.

The IMEs of the predicted plumes were smaller than IMEs from their corresponding labeled plumes with one exception (Table 1). When averaged together, the predicted methane plumes captured 87% by mass of what the manual labels identified. Therefore, while the FCN is missing more than 50% of pixels manually labeled as methane, it is accurately identifying the majority of each plume by mass. Plume pixels not detected by the FCN are dominantly low enhancement and difficult to distinguish from background. False positive enhancements in the matched filter input caused by roads, roofs, and desert were accurately identified as not methane plumes.

Point source emitters can be intermittent[11], therefore target point sources in a time series will not always contain a methane plume. To address this issue, future FCNs will be trained on a time series dataset that contains scenes with and without plumes. This should make the FCN resistant to false positives close to point sources that have intermittent plumes.

The FCN generated by this research was trained on a very small dataset, yet produced good results. Deep learning applications greatly benefit from a large amount of data to train on. As larger time series datasets become available, the corresponding networks will likely increase in accuracy as well.

Table 1. IME calculations for plumes in the test dataset and the ratio of U-Net derived IME to manual label derived IME.

Plume IMEs

Flight-line	Labeled IME (kg)	U-Net IME (kg)	Ratio
ang20180917t212127	0.50	0.35	0.70
ang20180917t213701	1.57	1.47	0.94
ang20180917t192118	0.34	0.22	0.65
ang20180917t203546	0.79	0.94	1.19
		Average Ratio:	0.87

Table 2. FCN metrics. All metrics calculated with a 60% FCN prediction threshold.

FCN Metrics

Binary Accuracy	0.999
Precision	0.835
Recall	0.412
AUC	0.873

Results

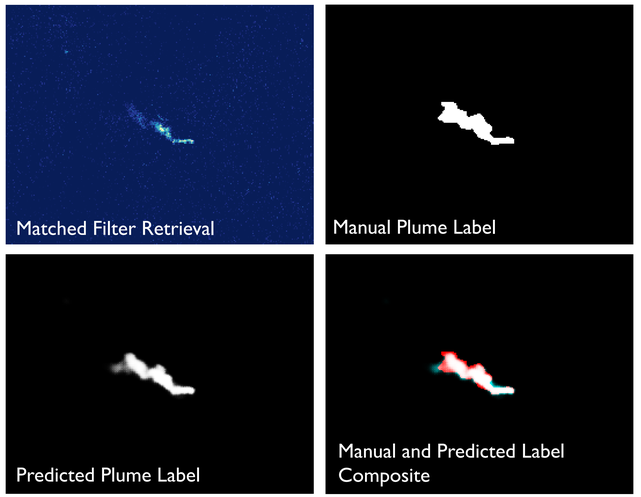

Figure 3. Methane plume images from flight-line ang20180917t213701

Figure 4. Manual and predicted label composites for flight-lines ang20180917t192118 and ang20180917t203546

True Positive False Positive False Negative True Negative

Conclusions

A FCN was successfully trained to delineate methane plumes from RGB and matched filter time series data. IMEs derived from the predicted plume labels were slightly smaller than IMEs calculated using manual labels. Persistent false positives in the matched filter data were rarely identified as plumes by the FCN. The success of this research presents an exciting case for utilizing deep learning to accurately delineate methane plumes as time series data for point source emitters becomes more readily available.

References

1. Myhre, G., Shindell, D., Bréon, F. M., Collins, W., Fuglestvedt, J., Huang, J., Koch, D., Lamarque, J.-F., Lee, D., Mendoza, B., Nakajima, T., Robock, A., Stephens, G., Takemura, T., Zhang, H. (2013). Anthropogenic and natural radiative forcing. *Climate Change*, 423, 658-740.
2. Saunois, M., Bousquet, P., Poulter, B., Peregon, A., Ciais, P., Canadell, J. G., ... & Zhu, Q. (2016). The global methane budget 2000–2012. *Earth System Science Data*, 8(2), 697-751.
3. Varon, D. J., McKeever, J., Jervis, D., Maasakkers, J. D., Pandey, S., Houweling, S., et al. (2019). Satellite discovery of anomalously large methane point sources from oil/gas production. *Geophysical Research Letters*, 46 (22), 13507–13516.
4. Duren, R. M.; Thorpe, A. K.; Foster, K. T.; Rafiq, T.; Hopkins, F. M.; Yadav, V.; Bue, B. D.; Thompson, D. R.; Conley, S.; Colombi, N. K.; Frankenberg, C.; McCubbin, I. B.; Eastwood, M. L.; Falk, M.; Herner, J. D.; Croes, B. E.; Green, R. O.; Miller, C. E. California's methane super-emitters. *Nature* 2019, 575, 180– 184.
5. Frankenberg, C., Thorpe, A. K., Thompson, D. R., Hulley, G., Kort, E. A., Vance, N., ... & Green, R. O. (2016). Airborne methane remote measurements reveal heavy-tail flux distribution in Four Corners region. *Proceedings of the National Academy of Sciences*, 113(35), 9734-9739.
6. Varon, D. J., Jacob, D. J., McKeever, J., Jervis, D., Durak, B. O. A., Xia, Y., & Huang, Y. (2018). Quantifying methane point sources from fine-scale satellite observations of atmospheric methane plumes. *Atmospheric Measurement Techniques*, 11 (10), 5673–5686.
7. Ayasse, A. K., Dennison, P. E., Foote, M., Thorpe, A. K., Joshi, S., Green, R. O., et al. (2019). Methane mapping with future satellite imaging spectrometers. *Remote Sensing*, 11 (24), 3054.
8. Ma, L., Liu, Y., Zhang, X., Ye, Y., Yin, G., & Johnson, B. A. (2019). Deep learning in remote sensing applications: A meta-analysis and review. *ISPRS Journal of Photogrammetry and Remote Sensing*, 152, 166–177.
9. Kattenborn, T., Leitloff, J., Schiefer, F., & Hinz, S. (2021). Review on convolutional neural networks (CNN) in vegetation remote sensing. *ISPRS Journal of Photogrammetry and Remote Sensing*, 173, 24–49.
10. Ronneberger, O., Fischer, P., & Brox, T. (2015). U-net: Convolutional networks for biomedical image segmentation. *In International Conference on Medical Image Computing and Computer-assisted Intervention* (pp. 234-241). Springer, Cham.
11. Cusworth, D. H., Duren, R. M., Thorpe, A. K., Olson-Duvall, W., Heckler, J., Chapman, J. W., Eastwood, M. L., Helmlinger, M. C., Green, R. O., Asner, G. P., Dennison, P. E., & Miller, C. E. (2021). Intermittency of large methane emitters in the Permian Basin. Environmental Science & Technology Letters, 8 (7), 567–573

Acknowledgements

Funding for this research was provided by NASA Carbon Monitoring System Grant 80NSSC20K0244. We acknowledge the support and effort of the NASA JPL AVIRIS-NG team.